A Review Paper

Occipitocervical Junction: Imaging, Pathology, Instrumentation

Michael Benke, MD, Warren D. Yu, MD, Sean C. Peden, MD, and Joseph R. O'Brien, MD, MPH

Abstract

The occipitocervical junction (OCJ) is a highly specialized area of the spine. Understanding the unique anatomy, imaging, and craniometry of this area is paramount in recognizing and managing the potentially devastating effects that pathology has on it. Instrumentation techniques continue to evolve, the goal being to safely obtain durable, rigid constructs that allow immediate stability, anatomical alignment, and osseous fusion. This article reviews the pathologic conditions at the OCJ and the current instrumentation and fusion options available for treatment. The general orthopedist needs to recognize the pathology common in this region and appropriately refer patients for treatment.

The occipitocervical junction (OCJ) is the unique set of articulations among the occipital bone or occiput (C0), the atlas (C1), and the axis (C2). This anatomical area is also known as the craniovertebral junction; in the literature, the 2 terms are used interchangeably. The OCJ lacks intervertebral disks and depends on strong capsular and ligamentous attachments for stability.[1] This region affords a large degree of mobility, with about half of all cervical flexion-extension coming from C0–C1 and half of all cervical rotation occurring at C1–C2.[1] Recognition and treatment of OCJ pathology require a thorough understanding of osseous, ligamentous, and neurovascular anatomy. Understanding imaging and associated craniometry of the OCJ is paramount. General orthopedists needs to recognize the pathology common in this region and appropriately refer patients for treatment.

Dr. Benke is Resident, Department of Orthopaedic Surgery, George Washington University, Washington, DC.
Dr. Yu is Chief, Spine Section, Department of Orthopaedic Surgery, George Washington University Hospital, and Associate Professor of Orthopaedic Surgery and Neurosurgery, George Washington University School of Medicine, Washington, DC.
Dr. Peden is Resident, Department of Orthopaedic Surgery, George Washington University.
Dr. O'Brien is Associate Director of Spine Surgery, George Washington University Hospital, and Assistant Professor, George Washington University School of Medicine.

Address correspondence to: Sean C. Peden, MD, 2150 Pennsylvania Avenue NW, 7th Floor, Washington, DC 20037 (tel, 203-918-0409; e-mail, sean.peden@gmail.com).

Am J Orthop. 2011;40(10):E205-E215.

Anatomy

The occiput, a wide, flat bone at the posteroinferior aspect of the skull, encases the cerebellum, the pons, and the medulla in the posterior fossa. The sphenoid bone also makes up part of the posterior fossa as it articulates with the anterior border of the occiput. The clivus (Latin for "slope") is the superior portion of the sphenoid bone that meets the portion of the occiput anterior to the foramen magnum (Figure 1). Through the foramen magnum, a large, oval aperture in the occiput, the cranium communicates with the vertebral canal. The foramen magnum is bound anteriorly by the basion, posteriorly by the opisthion, and laterally by the convex occipital condyles; it transmits the medulla oblongata, the spinal accessory nerves (CN11), the vertebral arteries, the anterior and posterior spinal arteries, the tectorial membrane, and the alar ligaments. The hypoglossal nerve (CN12) courses through the hypoglossal canal in the base of each occipital condyle.[2]

The atlas (C1) is a ring-shaped vertebra composed of right and left lateral masses connected by anterior and posterior arches. The atlas has no vertebral body. The C1 lateral masses articulate superiorly with the occipital condyles and inferiorly with the C2 superior articular facets. The dens (a.k.a. odontoid process) of C2 articulate with the posterior surface of the anterior arch of C1 and is held in place by strong ligamentous attachments to the atlas and the skull (Figure 2). Craniocervical instability can originate at the C0–C1 and C1–C2 joints.[3]

The unique combination of motion and stability at the OCJ is provided by its strong ligamentous structures.[4-6]

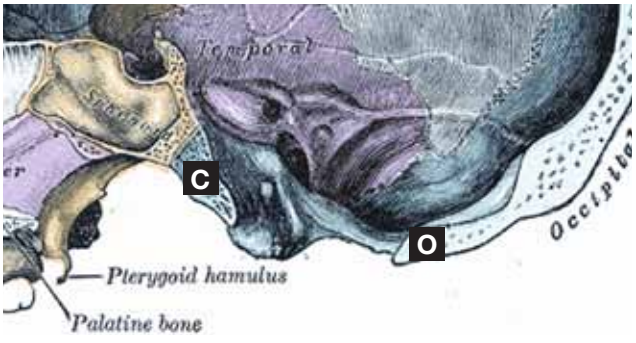

Figure 1. Coned-down cross-section of skull shows important anatomical structures and their relationships in occipitocervical junction. Clivus (C) is posterior portion of sphenoid bone, with smooth inferior slope. Occipital bone (occiput) makes up posterior rim of foramen magnum. The anterior point of occiput—posterior margin of foramen magnum at its midpoint—is opisthion (O). Courtesy of *Gray's Anatomy of the Human Body.* 20th US ed. Public domain.

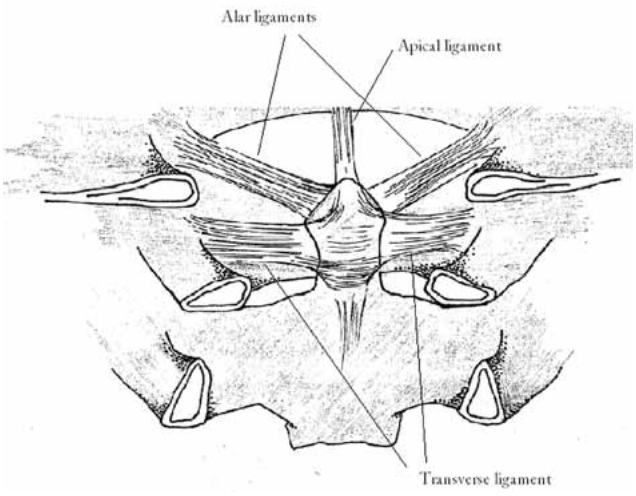

Figure 2. Sketch of odontoid peg and its major ligaments attaching to occiput (C0) and atlas (C1). Posterior elements have been removed. The tectorial membrane, a continuation of the posterior longitudinal ligament, has been removed to better expose these ligaments.

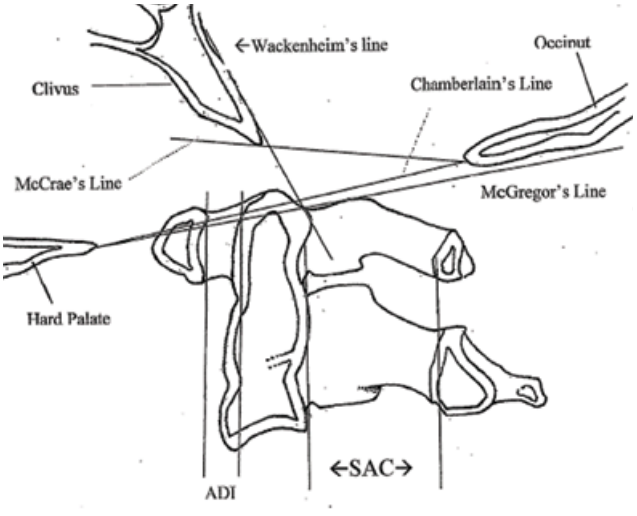

Figure 3. Cross-sectional view of occipitocervical junction (OCJ). The following parameters are often used when interpreting sagittal computed tomography scan or lateral radiograph for signs of pathology at OCJ. Dens should remain below Wackenheim line, which is drawn as tangent to posterior slope of clivus. McRae line connects tip of clivus to opisthion, and protrusion of dens above it is abnormal. Chamberlain and McGregor lines use hard palate as reference point for 2 additional lines, and protrusion of dens 3 mm above Chamberlain line and 4.5 mm above McGregor line is abnormal. Atlantodental interval (ADI; sometimes anterior ADI [AADI]), is usually less than 3 mm in adults and 5 mm in children. At this spinal level, minimum space available for cord (SAC) to avoid compression is 14 mm.

Anteriorly, the OCJ is stabilized by 5 ligaments—the anterior atlanto-occipital membrane (continuation of anterior longitudinal ligament), the tectorial membrane (continuation of posterior longitudinal ligament), the transverse ligament (secures dens to anterior arch of C1), the alar ligaments (connect dens to occipital condyles and are the main restraints to axial rotation and lateral bending[4,5]), and the

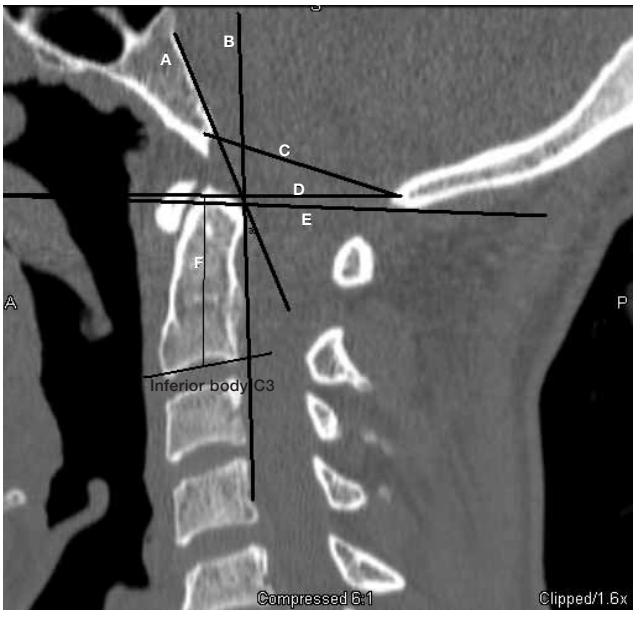

Figure 4. Midline sagittal computed tomography of normal anatomy. Hard palate is commonly not well visualized on neck CT. Wackenheim clivus baseline (A), posterior axial line or posterior vertebral line (B), and angle that they form, clivus–canal angle (a), are shown. McRae line (C), Chamberlain line (D), and McGregor line (E) are also shown. Lines are drawn to demonstrate Redlund-Johnell criterion. Distance from inferior body of axis (C2) to McGregor line (F) should be less than 29 mm in women or less than 34 mm in men.

apical ligament (connects dens to basion). The posterior stabilizing structures are the ligamentum nuchae, the interspinous ligament, the posterior atlanto-occipital membrane, the ligamentum flavum, and the cervical musculature.[4-6]

Occipitocervical Craniometry

Pathologic conditions at the OCJ may be evaluated with conventional radiography, computed tomography (CT), and magnetic resonance imaging (MRI). Anatomical landmarks, parameters, and relationships that were originally described on conventional radiography,[7-9] and that form the basis for occipitocervical craniometry, have been extrapolated for use with CT and MRI (Table).

The Wackenheim clivus baseline is a tangent along the superior surface of the clivus[10] (Figure 3). Extension of the tip of the dens above or posterior to this line is abnormal and indicates basilar invagination. The clivus–canal angle is formed by the Wackenheim clivus baseline and the posterior vertebral body line. The normal range is 180° in extension to 150° in flexion. Ventral spinal cord compression may occur when the angle is less than 150°.[11]

The McRae line runs from the basion to the opisthion (protrusion of tip of dens above line is abnormal[12,13]), the Chamberlain line from the hard palate to the opisthion (protrusion of dens more than 3 mm above line is abnormal[8]), and the McGregor line from the hard palate to the most caudal aspect of the occiput on midsagittal images (protru-

Table. Radiographic Parameters of Occipitocervical Junction

Eponym	Parameters	Pathology
Wackenheim clivus baseline	Tangent drawn along superior surface of clivus	Dens should be below line
Clivus–canal angle	Angle formed by Wackenheim line and posterior vertebral body line	Normal range is 180° in extension to 150° in flexion; angle of <150° is abnormal
McRae line	From basion to opisthion	Protrusion of dens above line is abnormal
Chamberlain line	From hard palate to opisthion	Protrusion of dens >3 mm above line is abnormal
McGregor line	From hard palate to most caudal point on midline occipital curve	Protrusion of dens >4.5 mm above line is abnormal
Ranawat criterion	Distance from center of pedicle of C2 to transverse axis of C1	<15 mm in men or <13 mm in women is abnormal
Redlund-Johnell criterion	Distance from inferior C2 body to McGregor line	<34 mm in men or <29 mm in women is abnormal
Welcher basal angle	Tangent to clivus as it intersects tangent to sphenoid bone	Normal range is 125°-143°; platybasia occurs when basal angle is >143°
Basion–dens interval	From tip of basion to tip of dens	>12 mm is abnormal
Basion–atlanto interval	From tip of basion to posterior axial line of C2	>12 mm is abnormal
Powers ratio	Ratio of line from basion to posterior arch of C1 (BP) to line from opisthion to anterior arch of C1 (OA)	>1.0 is abnormal
Anterior atlantodental interval	From anterior arch of C1 to dens	>3 mm in adults or >4.5-5 mm in children is abnormal
Posterior atlantodental interval	From dens to posterior arch of C1	<14 mm is abnormal
Atlanto-occipital joint axis angle	Angle formed by lines drawn parallel to atlanto-occipital joints on coronal images	Normal range is 124°-127°

sion of dens more than 4.5 mm above line is abnormal[9]). Use of these lines on conventional lateral radiographs may be limited by difficulty in identifying the hard palate and the margin of the opisthion (Figure 4).

The Ranawat criterion uses the distance between the center of the second cervical pedicle and the transverse axis of C1 measured along the axis of the dens on lateral radiographs. A distance of less than 15 mm in men or less than 13 mm in women is abnormal and indicates basilar invagination[14] (Figure 5).

The Redlund-Johnell criterion uses the distance between the McGregor line and the midpoint of the inferior margin of the C2 vertebral body as measured along the axis of the dens. A distance of less than 34 mm in men or less than 29 mm in women is abnormal and indicates basilar invagination.[7]

The Welcher basal angle can be used to measure platybasia, or abnormal flattening of the skull base. Platybasia is associated with OCJ abnormalities, such as occipitalization of the atlas and basilar invagination, and can occur in a variety of congenital disorders (osteogenesis imperfecta, cranio-cleidodysostosis) or acquired diseases (Paget disease, osteomalacia, rickets, trauma).[15] The basal angle is formed by a tangent to the clivus (Wackenheim line) and a line tangent to the sphenoid bone. Platybasia is defined as a basal angle of more than 143° (normal range, 125°-143°) (Figure 6).

On conventional radiographs, none of these measurements have a sensitivity or negative predictive value of more than 90%.[16] Therefore, if there is any suggestion of cranial settling on plain radiographs, advanced imaging studies (CT, MRI) should be used to investigate.[16] The criteria described as relevant to radiographs are applicable to both CT and MRI.[16,17]

Several parameters can be used to predict atlanto-occipital dissociation (AOD). The basion–dens interval (BDI) is the distance from the tip of the basion to the tip of the dens. The basion–atlas interval (BAI) is the distance of the transverse line from the tip of the basion to the posterior axial line of C2. BDI or BAI of more than 12 mm is abnormal.[18] The Powers ratio, described by Powers and colleagues[19] in 1979, is the ratio of the distances of 2 lines (Figures 7, 8). Line BP is measured from the basion to the posterior arch of C1, and line OA is measured from the opisthion to the anterior arch of C1. A Powers ratio (BP:OA) of more than 1.0 is abnormal and indicates AOD.[19]

The anterior atlantodental interval is the distance from the anterior arch of C1 to the dens. A distance of more than

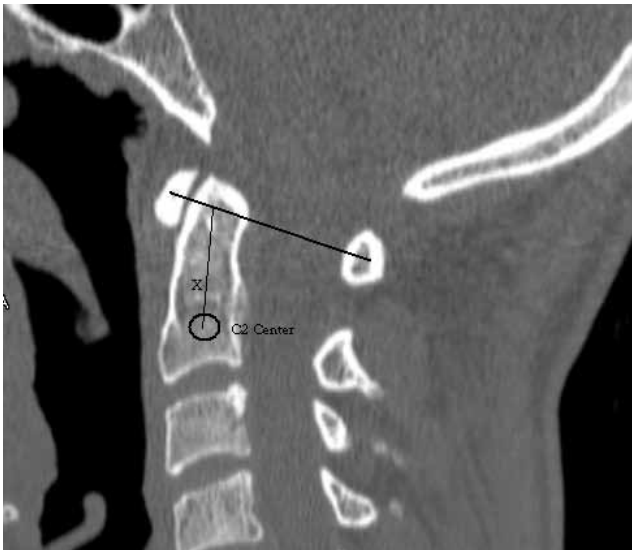

Figure 5. Normal midsagittal computed tomography shows Ranawat criterion. Circle represents center of C2 pedicle. Line is drawn (x) from center of circle to transverse axis of atlas (C1). Length of line (x) should be less than 13 mm in women or less than 15 mm in men.

3 mm in adults or more than 4.5 mm or 5 mm in children is abnormal and indicates atlantoaxial subluxation. The posterior atlantodental interval (PADI, a.k.a. space available for the cord) is the distance between the posterior surface of the dens and the anterior margin of the posterior arch of C1. This direct measurement of the spinal canal is used to assess atlantoaxial subluxation. A minimum of 14 mm is required to avoid cord compression[20] (Figure 9).

The atlanto-occipital joint (AOJ) axis angle is formed by lines drawn parallel to the AOJs on the coronal images. These lines typically intersect at the center of the dens when the condyles are symmetric. The normal range is between 124° and 127°. A wider, more obtuse angle indicates occipital condyle hypoplasia[21] (Figure 10).

Pathology

Pathologic conditions at the OCJ may compromise normal anatomical relationships and can lead to superior migration of the dens, atlantoaxial instability, and neural compression. Several terms arise in discussions of craniocervical instability, and they should not be used interchangeably. Basilar invagination differs from basilar impression, which differs from cranial settling. Basilar invagination refers to superior protrusion of the dens and loss of skull height secondary to congenital abnormalities. Basilar impression is secondary to skull-base softening caused by an acquired condition, such as Paget disease or osteomalacia. Cranial settling refers to vertical subluxation of the dens caused by loss of ligamentous support structures. Cranial settling can occur with rheumatoid or psoriatic arthritis.

Primary/Congenital Conditions

Congenital conditions of the occiput, atlas, and axis can lead to basilar invagination and brain-stem compression.[17,22]

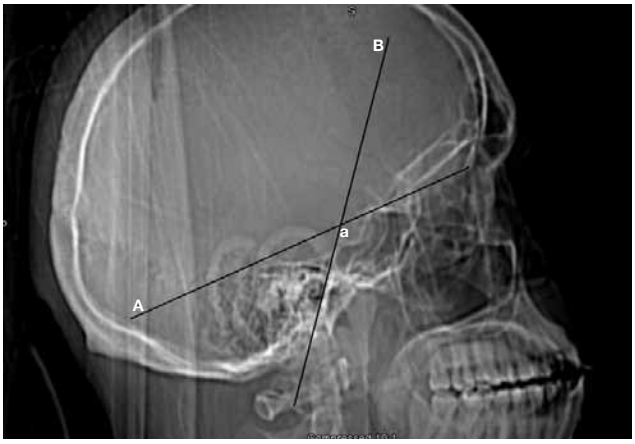

Figure 6. Lateral radiograph of normal skull. Line A is tangent to sphenoid, line B tangent to clivus. Angle formed (a) should be between 125° and 143°.

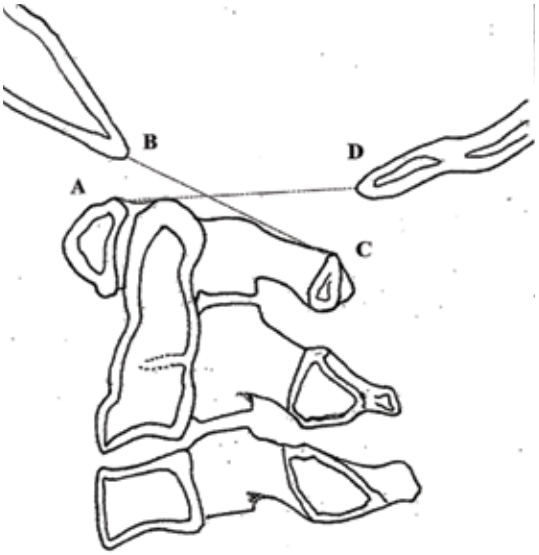

Figure 7. Sketch of occipitocervical junction. Powers ratio is useful in diagnosing atlanto-occipital dissociation. Distance from basion (B) to posterior arch of atlas (C1) (C) is divided by distance from anterior arch of C1 (A) to opisthion (D). BC/AD larger than 1 indicates atlanto-occipital dissociation.

Congenital Anomalies of Occiput. Congenital conditions of the occiput may be secondary to failure of formation (hypoplastic) or failure of segmentation.[11,12] Hypoplastic disorders of the occiput include basioccipital hypoplasia and occipital condyle hypoplasia.[11,22] Basioccipital hypoplasia is caused by failure of formation of the 4 occipital sclerotomes—which results in a shortened or hypoplastic clivus and, often, basilar invagination, best measured with the Chamberlain line.[22] Occipital condyle hypoplasia leads to short, flat condyles, which in turn, lead to limited AOJ motion and basilar invagination. Although the deformity is usually bilateral, unilateral cases have been reported.[21,22]

Failure of segmentation between the skull and the first cervical vertebra results in atlanto-occipital assimilation (Figure 11), which may be complete or partial and invari-

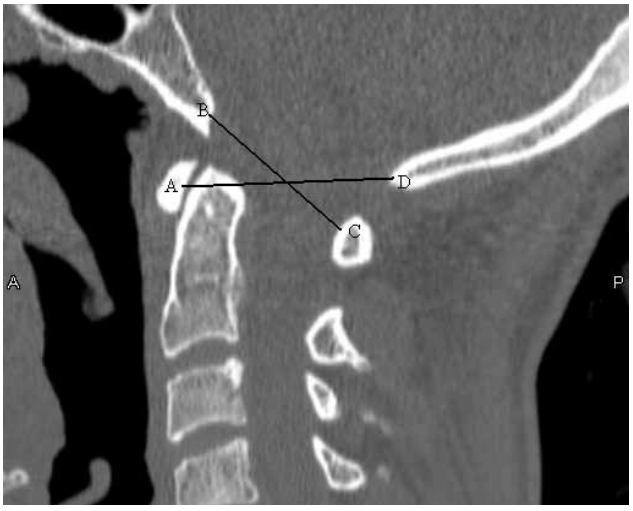

Figure 8. Midsagittal computed tomography of occipitocervical junction sketched in Figure 7. Powers ratio is useful in diagnosing atlanto-occipital dissociation. Distance from basion (B) to posterior arch of atlas (C1) (C) is divided by distance from anterior arch of C1 (A) to opisthion (D). BC/AD larger than 1 indicates atlanto-occipital dissociation.

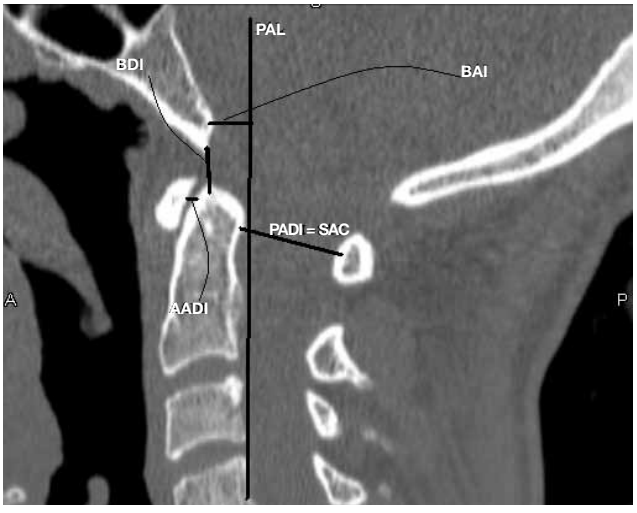

Figure 9. Midsagittal computed tomography of normal patient shows basion–dens interval (BDI), basion-atlanto interval (BAI), anterior atlantodental interval (AADI), and posterior atlantodental interval (PADI). BDI is from basion to tip of dens. BAI is from basion to line representing posterior axial line (line tangent to posterior surface of axis, C2). Both should be less than 12 mm. AADI is from anterior ring of atlas (C1) to dens. PADI or SAC (space available for cord) is from posterior ring of C1 to dens.

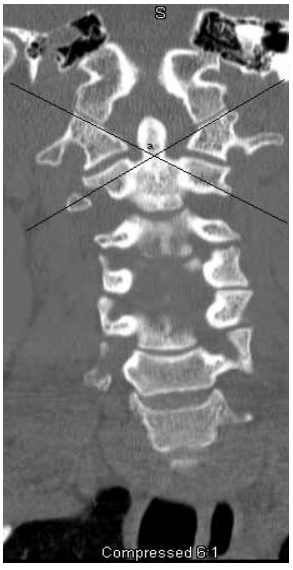

Figure 10. Coronal computed tomography of normal patient shows occipitocervical junction. Atlanto-occipital angle is formed by lines drawn parallel to both atlanto-occipital joints on coronal image. Angle formed by these intersecting lines should be between 124° and 127°. When symmetric, lines should intersect midline.

Figure 11. Parasagittal computed tomography of adult with congenital atlanto-occipital assimilation. As there is no joint space between occipital condyles and superior articular process of atlas (C1), basilar invagination often results.

ably results in basilar invagination.[22] Clinically, patients may present with a stiff neck or pain after minor trauma. Restricted range of motion at C0–C1 may lead to instability at C1–C2. Almost 50% of patients with atlanto-occipital assimilation develop C1–C2 instability and myelopathy by the third decade of life.[11-13,23]

Congenital Anomalies of Atlas. With the exception of atlanto-occipital assimilation, most anomalies of the atlas do not alter OCJ anatomical relationships and are not associated with basilar invagination.[24] As the atlas does not have a true spinous process, failure of formation at the atlas is referred to as rachischisis rather than spina bifida of C1.[22] Posterior arch clefts of the atlas, the most common pattern, are found in 4% in autopsy specimens.[25,26] Most of posterior arch clefts are midline (97%); lateral clefts through the sulcus for the vertebral artery account for 3% of posterior arch clefts.[25,26] Posterior arch rachischisis may be mistaken for dens fracture when superimposed on an open-mouth-view radiograph.[24] Anterior arch clefts are much less common; they are found in 0.1% of autopsy specimens.[25,26] When associated with a posterior cleft, the so-called split atlas may mimic a Jefferson fracture.[27] Well-corticated margins and lack of posterior tubercle may help differentiate these 2 conditions.[22,25-27]

Congenital Anomalies of Axis. Most congenital anomalies of the axis are confined to the dens and usually are not associated with basilar invagination,[22] though they may result in atlantoaxial instability.[28] Like anomalies of the atlas, these also may mimic fracture. Knowledge of axis ossification centers aids in understanding the anomalies.[29] The dens has 3 ossification centers—2 columnar centers, which ossify before birth and form the body of the dens, and 1 center at the tip of the dens.

Persistent ossiculum terminale (a.k.a. the Bergman ossicle), which results from failure of fusion of the terminal ossicle of the dens,[22] may be mistaken for a type I dens fracture[30] and has little clinical consequence.[22] The dentocentral synchondrosis normally fuses by age 6. Os odontoideum results from failure of fusion or fracture of the dentocentral

Figure 12. (A) Lateral radiograph of adult with os odontoideum. Note hypertrophic rounded anterior arch of atlas (C1). (B) Open-mouth dens radiograph confirms this diagnosis.

Figure 13. (A) Radiograph of patient with rheumatoid arthritis demonstrates cranial settling. (B) C1-C2 instability associated with rheumatoid arthritis. Note violation of Wackenheim clivus line.

synchondrosis. Although os odontoideum may be mistaken for a type II dens fracture, the well-corticated, convex upper margin of the C2 body and the hypertrophic, rounded anterior arch of C1 help differentiate these 2 conditions[24] (Figures 12A, 12B). Atlantoaxial instability is the hallmark of os odontoideum[22,28] and is associated with Down syndrome, spondyloepiphyseal dysplasia, Morquio syndrome, and other congenital diseases involving abnormalities of connective tissue.[31] Complete aplasia of the dens is exceedingly rare. Occasionally, an os odontoideum that projects perfectly over the arch of the atlas on open-mouth radiograph may be confused for odontoid aplasia.[24]

Acquired Conditions

Acquired conditions include Paget disease, osteomalacia, rickets, osteogenesis imperfecta, and neurofibromatosis, all of which soften the skull base.[22] When one of these conditions causes skull-base softening and superior dens migration, the term basilar impression is used. Alternatively, when an acquired disease such as rheumatoid arthritis (RA) causes destruction of OCJ ligamentous structures, and leads to vertical subluxation of the dens, the term cranial settling is used.[17,22]

Rheumatoid and Psoriatic Arthritis. RA is a chronic, systemic inflammatory disorder that principally attacks the synovial joints and produces a synovitis that progresses to destruction of the articular cartilage and ankylosis. The synovial joints develop an inflammatory pannus that erodes supporting ligamentous structures through generated cytokines.[11,20,22] Psoriatic arthritis develops in 1% to 2% of patients with psoriasis and affects the synovial joints in a similar manner.

In the cervical spine, the OCJ and the subaxial cervical spine are often affected.[20,22,32,33] Most commonly, erosion of the ligaments at the OCJ leads to atlantoaxial instabil-

Figure 14. Open-mouth dens radiograph of trauma patient. Jefferson fracture of atlas (C1) is evident in overhang of C1 lateral masses on C2.

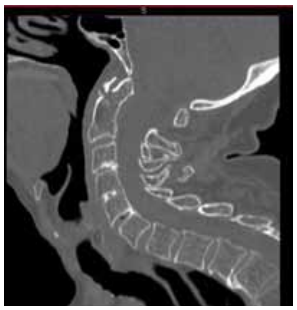

Figure 15. Sagittal computed tomography of trauma patient reporting neck pain. Angulated type II dens fracture is evident.

ity.[20,32] Progression of the disease leads to erosion of the lateral masses of C1 and then of the occipital condyles and facets of C2. This erosion results in cranial settling and can cause myelopathy, increased intracranial pressure, and various other neurologic deficits, including deficits involving the cranial nerves[20,22,32] (Figures 13A, 13B).

The method of Redlund-Johnell may be used to gauge settling.[7] As vertical subluxation occurs and the dens begins to occupy a more rostral position, the dens compresses the brain stem and vertebrobasilar system—which may result in sudden death in patients with advanced RA.[20,22,32] The risk for this catastrophic event must be evaluated before any surgery is performed in patients with RA. In 1993, Boden and colleagues[32] used PADI on MRI to predict recovery after cervical stabilization for atlantoaxial instability in rheumatoid patients (Figure 3). They found that PADI of less than 14 mm had a 97% positive predictive value in detecting patients with a neurologic deficit. Moreover, neurologic recovery after surgery was unlikely if PADI was less than 10 mm, but complete motor recovery occurred after surgery if PADI was more than 14 mm.[20,32,33]

Trauma to Occipitocervical Junction. Detailed discussion of trauma to the upper cervical spine is beyond the scope of this article. Here we give a brief overview of OCJ trauma with relevant radiographic findings.

Of the 34,069 blunt trauma patients described in a 2001 report, 2.4% had cervical spine injuries; 34% of these injuries occurred at the OCJ.[34] This relatively high incidence, combined with the devastating consequences of these injuries, highlights the importance of imaging and recognizing injury at the OCJ.[35,36]

In 2007, the Spine Trauma Study Group published a consensus statement on measurement techniques for upper cervical spine injuries.[37]

Atlanto-occipital Dissociation. AOD is a devastating and often fatal injury resulting from high-energy trauma. The cranium and spine are effectively separated, resulting in functional decapitation, with only surrounding soft tissue connecting the head to the body. The head most often displaces anteriorly, but posterior AOD also occurs. The spectrum of injury includes complete loss of articulation (dislocation) versus subluxation. With improvements in intensive care, the survival rates from this once certainly fatal injury are increasing. For various reasons, including increased cranial mass relative to the body, this injury is more common in the pediatric population.

The Harris technique, or the "rule of 12," is the most useful, sensitive, and reproducible technique for characterizing AOD.[37] This technique uses BDI and BAI. Harris and colleagues[18] found that BDI and BAI did not exceed 12 mm in 95% and 98% of adults, respectively. Fisher and colleagues[38] retrospectively assessed lateral radiographs of 37 patients who presented with a diagnosis of AOD. Both BDI and BAI were more than 12 mm in 23 patients with atlanto-occipital dislocation and in 8 patients with subluxation/dissociation. BDI and BAI were less than 12 mm in 6 patients who were initially suspected to be unstable but who did not have supportive clinical findings of AOD. In the same group of patients, the Powers ratio detected injury in only 60% of patients.[38] Although the Harris technique was described on lateral radiographs, midsagittal CT is recommended for diagnosis of AOD.

Occipital Condyle Fractures. Occipital condyle fractures are rare injuries. They were originally described postmortem in trauma victims. The hypoglossal canal is intricately associated with the occipital condyle. Therefore, a displaced fracture demands close cranial nerve examination. These fractures are classified on the basis of bony versus ligamentous involvement.[39] Larger bony fragments are generally more stable and have increased healing potential with nonoperative immobilization.[40] CT with parasagittal and coronal reconstructions is best able to characterize occipital condyle fractures.[41]

Trauma to Atlas. In 1920, Jefferson[41] was the first to describe an axial load injury to the atlas resulting in a burst fracture of C1. Stability can be assessed with an open-mouth conventional dens radiograph. In a classic cadaver study, Spence and colleagues[42] determined that a combined overhang of the lateral masses of C1 over C2 of more than 6.9 mm on open-mouth radiograph was associated with transverse ligament rupture and a relatively unstable Jefferson burst fracture (Figure 14). Heller and colleagues[43] warned that magnification of plain radiographs overestimates this displacement and that the transverse ligament should be considered intact if combined lateral mass displacement is less than 8.1 mm on open-mouth radiograph. Using calibrated coronal CT reconstructions precludes this consideration. In addition to open-mouth dens radiograph and coronal CT, axial T_2-weighted MRI can confirm injury to the transverse ligament.[37]

Trauma to Axis. The axis is the most commonly fractured cervical vertebra.[34,44] Twenty-four percent of cervical fractures secondary to blunt trauma involve C2, and one-third of these are dens fractures.[34] Lateral cervical radiography or midsagittal CT is used to characterize these fractures.[37] Fracture location, displacement, and angulation are important prognostic factors in fracture healing and thus help define treatment algorithms. Measurement of fracture translation is based on the anterior aspect of the dens fragment

Figure 16. Sagittal computed tomography of patient with history of breast cancer with metastasis to dens shows bicortical occipital fixation with plate construct.

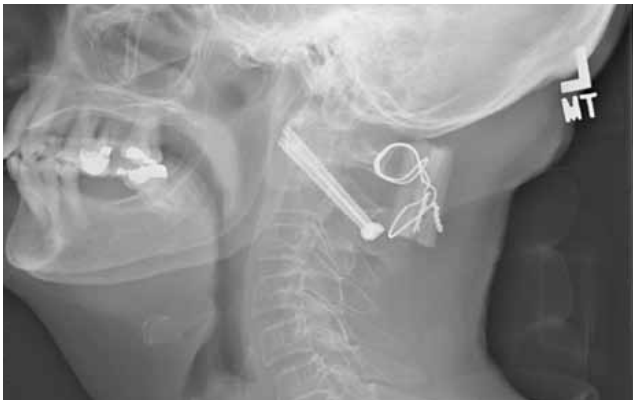

Figure 17. Postoperative lateral radiograph of patient with C1–C2 instability. C1–C2 transarticular screws (Magerl technique) are supplemented with posterior wire fixation.

and the anterior aspect of the C2 body. Fracture angulation is determined by the angle formed by a tangent line along the posterior aspect of the dens fragment and a tangent line along the posterior aspect of the C2 body (Figure 15). MRI is often helpful in determining the age of the fracture.

Traumatic Spondylolisthesis of Axis. In 1985, Levine and Edwards[45] described and classified their experience with traumatic spondylolisthesis of the axis, or hangman fracture. A hangman fracture consists of a pars interarticularis fracture and a C2–C3 disruption. The injury was originally associated with judicial hangings, but this injury often presents in patients with injury mechanisms involving far less traction and energy. Displacement and angulation, as visualized on midsagittal CT or plain radiography, are important in determining treatment.[37,45] Measurement of angulation can be based on lines drawn along the inferior endplates or on the posterior vertebral body lines of C2 and C3. Displacement is based on the posterior vertebral body lines drawn along the posterior aspect of C2 and C3.[45]

Instrumentation

Indications for instrumentation and fusion at the OCJ include instability secondary to trauma, RA, neoplasm, infection, congenital anomaly, and degenerative process. Surgical goals include decompression of neurologic structures as necessary, anatomical alignment, immediate rigid stability, and osseous fusion.

Historical Perspective

The evolution of occipitocervical fusion began in 1927 with a description by Foerster[46] of the use of a fibular strut graft to span the OCJ. Afterward, other techniques of onlay bone grafting, with and without wiring, were used to obtain fusion at the OCJ. Although modest fusion rates can be obtained, immediate stability is not a feature of this fixation method, and prolonged postoperative immobilization was required. This technique also carried the significant and obvious risks of wiring that violated the spinal canal.

Occipitocervical fixation with wires and hooks gave way to internal fixation with plates and screws. In 1999, Oda and colleagues[47] found that, compared with sublaminar hooks and wires, C2 transpedicular screws and C1–C2 transarticular screws provided statistically significant increased stability to an occipitocervical construct. Early occipital plating techniques, however, had various shortcomings including fixed hole distances leading to suboptimal screw placement.

Whereas screws provide excellent fixation at the OCJ and continue to evolve, plating of the upper cervical spine gave way to plate–rod constructs. Rods allow for optimal screw placement, compression or distraction across segments, and room for graft material.

Occipital Plating

Modern plates and locking screws allow for rigid, low-profile fixation at the occiput. The external occipital protuberance (attachment site of ligamentum nuchae and trapezius muscle) is the thickest part of the occiput and corresponds internally with the confluences of the sinuses. Occipital thickness decreases laterally and inferiorly from the external occipital protuberance.[48] Midline occipital fixation allows for longer screws with more pullout strength, and parasagittal screw placement allows for more screws with improved torsional strength.[49] Most contemporary plates allow for both midline and parasagittal screw placement. Biomechanically, bicortical fixation increases pullout strength (Figure 16). In an anatomical study of occipital morphology, Zipnick and colleagues[48] found that the outer and middle tables of the occipital skull contributed a total of 90% to overall bone thickness; the inner table contributed only 10%. Given the minimal contribution that the inner table made to bone thickness, the authors suggested that unicortical fixation is sufficient and lowers the risk for injury to the underlying venous sinuses.[48]

C0-C1 Transarticular Fixation

Transarticular instrumentation across the AOJ was first described by Gonzalez and colleagues[50] in 2003. Fluoroscopic imaging aids in placement of a screw from the lateral mass of C1 into the condyle of the occiput. Screw length should be kept under 28 mm to 32 mm to avoid violation of the

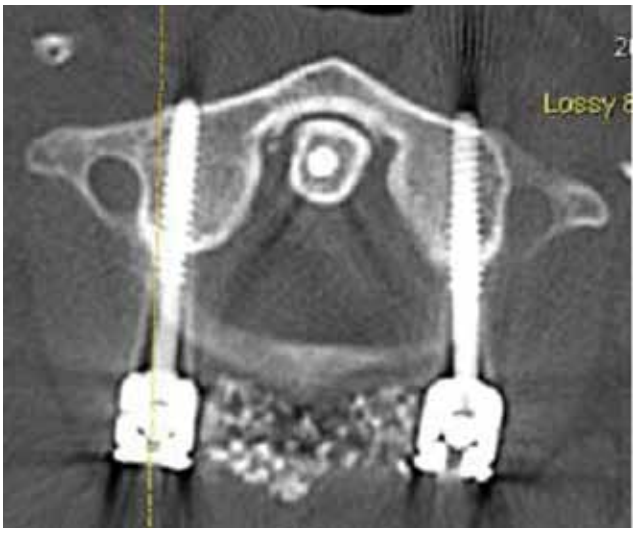

Figure 18. C1 lateral mass screws placed to treat a patient with failed anterior osteosynthesis of a type II odontoid fracture.

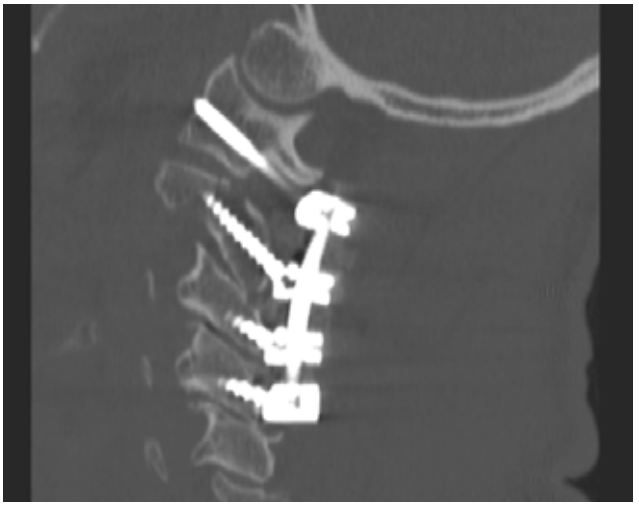

Figure 19. Sagittal computed tomography of a C2 pedicle screw.

hypoglossal canal in the base of the occipital condyle.[50]

Occipital Condyle Screw

Placement of screws in the occipital condyles for incorporation into rigid occipitocervical screw–rod constructs was recently described by La Marca and colleagues[51] in cadaveric models. The authors suggested that occipital condylar screws may be an alternative to conventional occipital fixation. After the occipitocervical musculature is elevated off the occiput and lamina of C1 and C2 in a standard posterior approach, the vertebral artery is located laterally, and its course is followed as it turns medially along the vertebral groove on the posterior arch of the atlas. The occipital condyle–C1 joint capsule is approximately 3 mm superior to the vertebral artery.[51] The hypoglossal canal and condylar emissary vein foramen lie rostrally in the occipital condyle, with the condylar emissary vein 8 mm to 10 mm superior to the

Figure 20. C2 lamina screws. As an alternative to pedicle screws, intralaminar screws are placed between inner and outer cortical table of C2 lamina in crossing fashion. Axial computed tomography shows patient with 4.0-mm screws in C2 lamina bilaterally.

inferior margin of the occipital condyle.[51] The entry point for screw insertion is 3 mm inferior to the emissary vein foramen in the midline of the condyle, between the medial foramen magnum and the extension of the lateral border of the occipital–C1 joint capsule.[51] La Marca and colleagues[51] successfully placed twelve 3.5×22-mm screws in 6 cadavers without violation of surrounding structures. In a 2009 case report, Uribe and colleagues[52] placed bilateral occipital condyle screws as part of a C0–C2 posterior occipitocervical fusion in a patient presenting with a delayed type II dens fracture with pseudarthrosis. Although this novel technique shows promise, challenging local anatomy with vital surrounding structures cannot be understated. In addition, clinical and biomechanical studies are lacking.

Atlanto-axial Instrumentation

Modern techniques for instrumentation at C1–C2 include C1–C2 transarticular screws, C1 lateral mass screws, C2 pedicle screws, and C2 translaminar screws. Screw fixation is biomechanically superior to semirigid sublaminar hooks or wires. Screws offer solid, 3-column fixation, producing stiffer constructs that may reduce the number of levels that require fusion.

In 1986, Magerl and Seemann[53] described transarticular screw fixation for atlantoaxial instability. Use of this technique led to fusion rates approaching 100%.[53] Although this technique is very powerful, it is also technically demanding. It requires preliminary reduction of C1 on C2 before screw insertion and poses a significant risk to the vertebral artery. Anatomical variants preclude use of this technique, at least on one side, in 20% of patients[54] (Figure 17).

An alternative to the Magerl transarticular screw technique for achieving C1–C2 fusion is the Harms technique,[54] which involves bilateral C1 lateral mass screws (Figure 18) and C2 pedicle screws (Figure 19) connected by rods. The

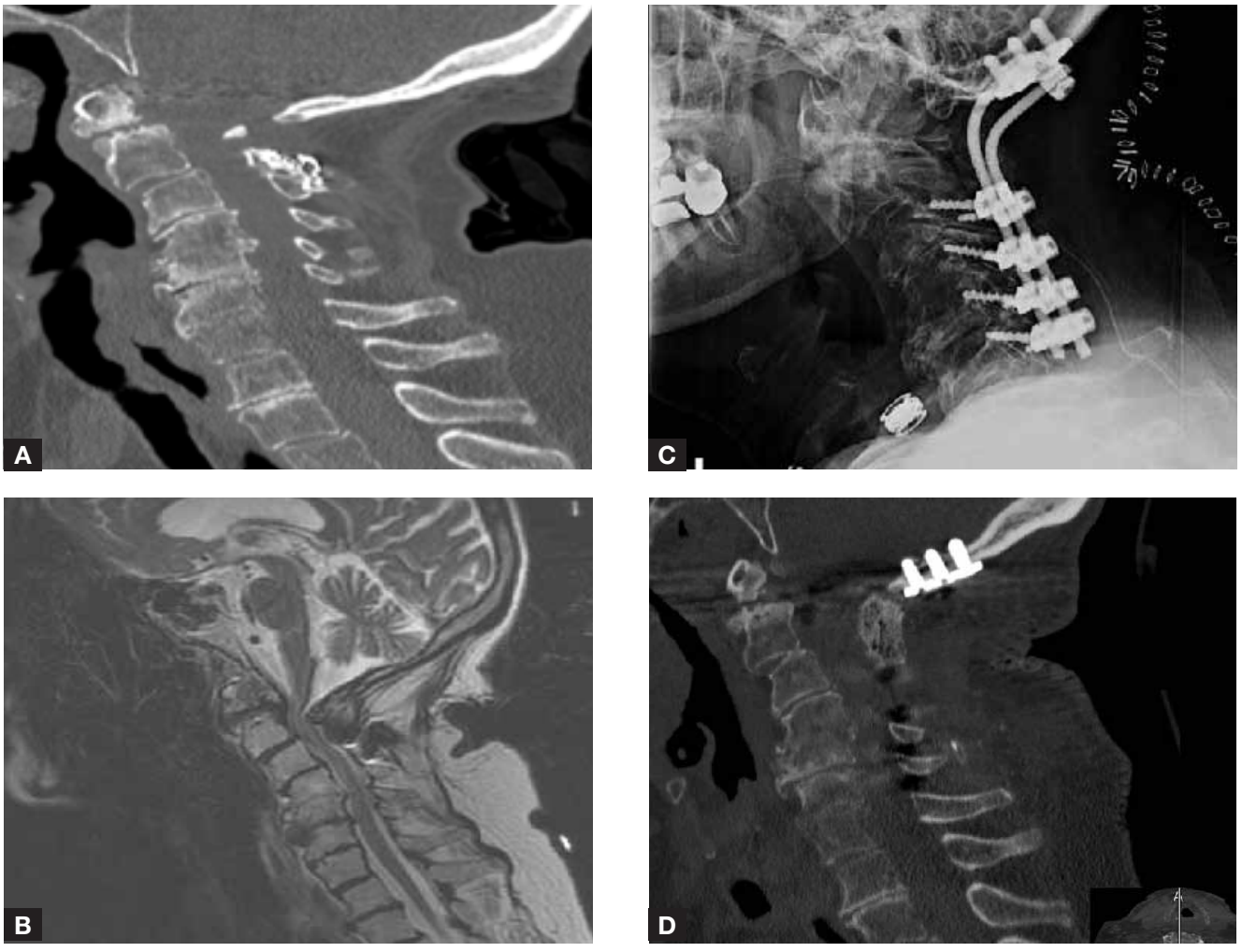

Figure 21. Five years after open reduction and internal fixation of C2 fracture, 86-year-old man presented with progressive difficulty walking and myelopathic signs. Midsagittal computed tomography (CT) (A) and magnetic resonance imaging (B) show previous wiring with significant stenosis and myelomalacia of occipitocervical junction. Postoperative radiograph (C) and CT (D) show combination of occipital plating and cervical screw-rod constructs combined with revision decompression.

lateral mass of C1 is large enough to accommodate 3.5-mm screws, and bicortical placement can be achieved safely. The C2 pedicle screws are placed through the pars interarticularis into the pedicle of the axis. Compared with transarticular screw placement, the more superior and medial trajectory decreases the risk to the vertebral artery.[54] In the original technique description, Harms and Melcher[54] obtained solid fusion without neural or vascular injury in 37 of 37 patients.

Pedicle screw placement in C2, however, remains technically challenging, and cadaveric studies have shown undesirably high rates of foramen transversarium violation.[55] In 2004, Wright[56] described a technique for C2 translaminar screw insertion as a safer alternative to instrumentation of the axis. Bilateral, crossing screws are placed between the inner and outer cortical tables of the lamina (Figure 20). This technique is relatively less demanding and diminishes the risk to the vertebral artery.[56] Care must be taken to not violate the ventral surface of the lamina and risk neurologic injury. Parker and colleagues[57] retrospectively reviewed placement of 161 C2 pedicle screws and 152 C2 translaminar screws in 167 patients. Eleven pedicle screws (7%) breached the pedicle, whereas only 2 translaminar screws (1.2%) breached the lamina. Fortunately, none of the misplaced pedicle screws caused catastrophic neurovascular injury. Biomechanical data from cadaveric studies suggest comparable rigidity of translaminar and pedicle screw constructs at C2,[58,59] yet several reports have questioned the clinical durability of translaminar screws, reporting higher rates of pseudarthrosis and hardware failure.[57,60] Long-term comparison studies, as well as biomechanical studies involving longer subaxial constructs, are lacking (Figures 21A–21D).

Conclusion

The OCJ is a highly specialized area of the spine. Understanding the unique anatomy, imaging, and craniometry of this area is paramount in recognizing and managing the potential devastating effects that pathology has on it. Instrumentation techniques continue to evolve, the goal being to safely obtain durable, rigid constructs that allow immediate stability, anatomical alignment, and osseous fusion.

Authors' Disclosure Statement and Acknowledgments

The authors report no actual or potential conflict of interest in relation to this article.

The authors would like to extend special thanks to Katherine Melvin Peden, Esq, for her help with the original illustrations and formatting. The authors would also like to acknowledge A. J. Khanna, MD for guidance in preparing this manuscript.

References

1. White AA III, Panjabi MM. The clinical biomechanics of the occipitoatlantoaxial complex. *Orthop Clin North Am*. 1978;9(4):867-878.
2. Moore KL, Dalley AF. *Clinically Oriented Anatomy*. Philadelphia, PA: Lippincott Williams & Wilkins; 1999.
3. Goel A. Treatment of basilar invagination by atlantoaxial joint distraction and direct lateral mass fixation. *J Neurosurg Spine*. 2004;1(3):281-286.
4. Dvorak J, Panjabi M, Gerber M, Wichmann W. CT-functional diagnostics of the rotatory instability of upper cervical spine. 1. An experimental study on cadavers. *Spine*. 1987;12(3):197-205.
5. Dvorak J, Schneider E, Saldinger P, Rahn B. Biomechanics of the craniocervical region: the alar and transverse ligaments. *J Orthop Res*. 1988;6(3):452-461.
6. Tubbs RS, Grabb P, Spooner A, Wilson W, Oakes WJ. The apical ligament: anatomy and functional significance. *J Neurosurg Spine*. 2000;92(2 suppl):197-200.
7. Redlund-Johnell I, Pettersson H. Radiographic measurements of the craniovertebral region. Designed for evaluation of abnormalities in rheumatoid arthritis. *Acta Radiol Diagn (Stockh)*. 1984;25(1):23-28.
8. Chamberlain WE. Basilar impression (platybasia). A bizarre developmental anomaly of the occipital bone and upper cervical spine with striking and misleading neurologic manifestations. *Yale J Biol Med*. 1939;11(5):487-496.
9. McGregor M. The significance of certain measurements of the skull in the diagnosis of basilar impression. *Br J Radiol*. 1948;21(244):171-181.
10. Wackenheim A. *Roentgen Diagnosis of the Cranio-Vertebral Region*. New York, NY: Springer-Verlag; 1974.
11. VanGilder JC, Menezes AH, Dolan KD. *The Craniovertebral Junction and Its Abnormalities*. Mount Kisco, NY: Futura; 1987.
12. McRae DL. Bony abnormalities in the region of the foramen magnum: correlation of the anatomic and neurologic findings. *Acta Radiol*. 1953;40(2-3):335-354.
13. McRae DL, Barnum AS. Occipitalization of the atlas. *Am J Roentgenol Radium Ther Nucl Med*. 1953;70(1):23-46.
14. Ranawat CS, O'Leary P, Pellicci P, Tsairis P, Marchisello P, Dorr L. Cervical spine fusion in rheumatoid arthritis. *J Bone Joint Surg Am*. 1979;61(7):1003-1010.
15. Koenigsberg RA, Vakil N, Hong TA, et al. Evaluation of platybasia with MR imaging. *AJNR Am J Neuroradiol*. 2005;26(1):89-92.
16. Riew KD, Hilibrand AS, Palumbo MA, Sethi N, Bohlman HH. Diagnosing basilar invagination in the rheumatoid patient. The reliability of radiographic criteria. *J Bone Joint Surg Am*. 2001;83(2):194-200.
17. Ross JS. Cervicomedullary and craniovertebral junctions. In: Modic MT, Masaryk TJ, Ross JS, eds. *Magnetic Resonance Imaging of the Spine*. St. Louis, MO: Mosby-Year Book; 1994:191-215.
18. Harris JH Jr, Carson GC, Wagner LK. Radiologic diagnosis of traumatic occipitovertebral dissociation: 1. Normal occipitovertebral relationships on lateral radiographs of supine subjects. *AJR Am J Roentgenol*. 1994;162(4):881-886.
19. Powers B, Miller MD, Kramer RS, Martinez S, Gehweiler JA Jr. Traumatic anterior atlanto-occipital dislocation. *Neurosurgery*. 1979;4(1):12-17.
20. Boden SD. Rheumatoid arthritis of the cervical spine. Surgical decision making based on predictors of paralysis and recovery. *Spine*. 1994;19(20):2275-2280.
21. Kunicki J, Ciszek B. The clinical anatomy and the occipital condyle variants [letter]. *Clin Anat*. 2005;18(8):646-647.
22. Smoker WR. MR imaging of the craniovertebral junction. *Magn Reson Imaging Clin North Am*. 2000;8(3):635-650.
23. Guille JT, Sherk HH. Congenital osseous anomalies of the upper and lower cervical spine in children. *J Bone Joint Surg Am*. 2002;84(2):277-288.
24. Smoker WR. Craniovertebral junction: normal anatomy, craniometry, and congenital anomalies. *Radiographics*. 1994;14(2):255-277.
25. Chambers AA, Gaskill MF. Midline anterior atlas clefts: CT findings. *J Comput Assist Tomogr*. 1992;16(6):868-870.
26. Gehweiler JA Jr, Daffner RH, Roberts L Jr. Malformations of the atlas vertebra simulating the Jefferson fracture. *AJR Am J Roentgenol*. 1983;140(6):1083-1086.
27. de Zoete A, Langeveld UA. A congenital anomaly of the atlas as a diagnostic dilemma: a case report. *J Manipulative Physiol Ther*. 2007;30(1):62-64.
28. Hensinger RN, Fielding JW. The cervical spine. In: Morrissy RT, ed. *Lovell and Winter's Pediatric Orthopaedics*. 3rd ed. Philadelphia, PA: Lippincott; 1990:703-739.
29. Copley LA, Dormans JP. Cervical spine disorders in infants and children. *J Am Acad Orthop Surg*. 1998;6(4):204-214.
30. Anderson LD, D'Alonzo RT. Fractures of the odontoid process of the axis. *J Bone Joint Surg Am*. 1974;56(8):1663-1674.
31. David KM, McLachlan JC, Aiton JF, et al. Cartilaginous development of the human craniovertebral junction as visualised by a new three-dimensional computer reconstruction technique. *J Anat*. 1998;192(pt 2):269-277.
32. Boden SD, Dodge LD, Bohlman HH, Rechtine GR. Rheumatoid arthritis of the cervical spine. A long-term analysis with predictors of paralysis and recovery. *J Bone Joint Surg Am*. 1993;75(9):1282-1297.
33. Dreyer SJ, Boden SD. Natural history of rheumatoid arthritis of the cervical spine. *Clin Orthop*. 1999;(366):98-106.
34. Goldberg W, Mueller C, Panacek E, Tigges S, Hoffman JR, Mower WR. Distribution and patterns of blunt traumatic cervical spine injury. *Ann Emerg Med*. 2001;38(1):17-21.
35. Adams VI. Neck injuries: I. Occipitoatlantal dislocation—a pathologic study of twelve traffic fatalities. *J Forensic Sci*. 1992;37(2):556-564.
36. Alker GJ Jr, Oh YS, Leslie EV. High cervical spine and craniocervical junction injuries in fatal traffic accidents: a radiological study. *Orthop Clin North Am*. 1978;9(4):1003-1010.
37. Bono CM, Vaccaro AR, Fehlings M, et al; Spine Trauma Study Group. Measurement techniques for upper cervical spine injuries: consensus statement of the Spine Trauma Study Group. *Spine*. 2007;32(5):593-600.
38. Fisher CG, Sun JC, Dvorak M. Recognition and management of atlanto-occipital dislocation: improving survival from an often fatal condition. *Can J Surg*. 2001;44(6):412-420.
39. Anderson PA, Montesano PX. Morphology and treatment of occipital condyle fractures. *Spine*. 1988;13(7):731-736.
40. Hanson JA, Deliganis AV, Baxter AB, et al. Radiologic and clinical spectrum of occipital condyle fractures: retrospective review of 107 consecutive fractures in 95 patients. *AJR Am J Roentgenol*. 2002;178(5):1261-1268.
41. Jefferson G. Fractures of the atlas vertebrae. *Br J Surg*. 1920;7:407-422.
42. Spence KF Jr, Decker S, Sell KW. Bursting atlantal fracture associated with rupture of the transverse ligament. *J Bone Joint Surg Am*. 1970;52(3):543-549.
43. Heller JG, Viroslav S, Hudson T. Jefferson fractures: the role of magnification artifact in assessing transverse ligament integrity. *J Spinal Disord*. 1993;6(5):392-396.
44. Ryan MD, Henderson JJ. The epidemiology of fractures and fracture-dislocations of the cervical spine. *Injury*. 1992;23(1):38-40.
45. Levine AM, Edwards CC. The management of traumatic spondylolisthesis of the axis. *J Bone Joint Surg Am*. 1985;67(2):217-226.
46. Foerster O. *Die Leitungsbahnen des Schmerzgefuhls und die chirurgishe Behandlung der Schmerzzustande*. Berlin, Germany: Urban & Schwarzenburg; 1927.
47. Oda I, Abumi K, Sell LC, Haggerty CJ, Cunningham BW, McAfee PC. Biomechanical evaluation of five different occipito-atlanto-axial fixation techniques. *Spine*. 1999;24(22):2377-2382.
48. Zipnick RI, Merola AA, Gorup J, et al. Occipital morphology. An anatomic guide to internal fixation. *Spine*. 1996;21(15):1719-1724.
49. Anderson PA, Oza AL, Puscak TJ, Sasso R. Biomechanics of occipitocervical fixation. *Spine*. 2006;31(7):755-761.
50. Gonzalez LF, Crawford NR, Chamberlain RH, et al. Craniovertebral junction fixation with transarticular screws: biomechanical analysis of a novel technique. *J Neurosurg*. 2003;98(2 suppl):202-209.
51. La Marca F, Zubay G, Morrison T, Karahalios D. Cadaveric study for placement of occipital condyle screws: technique and effects on surrounding anatomic structures. *J Neurosurg Spine*. 2008;9(4):347-353.
52. Uribe JS, Ramos E, Baaj A, Youssef AS, Vale FL. Occipital cervical stabilization using occipital condyles for cranial fixation: technical case report. *Neurosurgery*. 2009;65(6):E1216-E1217.
53. Magerl F, Seemann PS. Stable posterior fusion of the atlas and axis by transarticular screw fixation. In: Kehr P, Weidner A, eds. *Cervical Spine I*. New York, NY: Springer; 1986:322-327.
54. Harms J, Melcher RP. Posterior C1–C2 fusion with polyaxial screw and rod fixation. *Spine*. 2001;26(22):2467-2471.
55. Ebraheim N, Rollins JR Jr, Xu R, Jackson WT. Anatomic consideration of C2 pedicle screw placement. *Spine*. 1996;21(6):691-695.
56. Wright NM. Posterior C2 fixation using bilateral, crossing C2 laminar screws: case series and technical note. *J Spinal Disord Tech*. 2004;17(2):158-162.
57. Parker SL, McGirt MJ, Garcés-Ambrossi GL, et al. Translaminar versus pedicle screw fixation of C2: comparison of surgical morbidity and accuracy of 313 consecutive screws. *Neurosurgery*. 2009;64(5 suppl 2):343-348.
58. Reddy CH, Ingalhalikar AV, Channon S, Lim TH, Torner J, Hitchon PW. In vitro biomechanical comparison of transpedicular versus translaminar C-2 screw fixation in C2–3 instrumentation. *J Neurosurg Spine*. 2007;7(4):414-418.
59. Gorek J, Acaroglu E, Berven S, Yousef A, Puttlitz CM. Constructs incorporating intralaminar C2 screws provide rigid stability for atlantoaxial fixation. *Spine*. 2005;30(13):1513-1518.
60. Sciubba DM, Noggle JC, Vellimana AK, et al. Laminar screw fixation of the axis. *J Neurosurg Spine*. 2008;8(4):327-334.

This paper will be judged for the Resident Writer's Award.